ECOGRAPHY

Research article

Using computer vision to understand the global biogeography of ant color

Jacob H. Idec[®] 1, Tom R. Bishop[®] 2,3 and Brian L. Fisher[®] 4

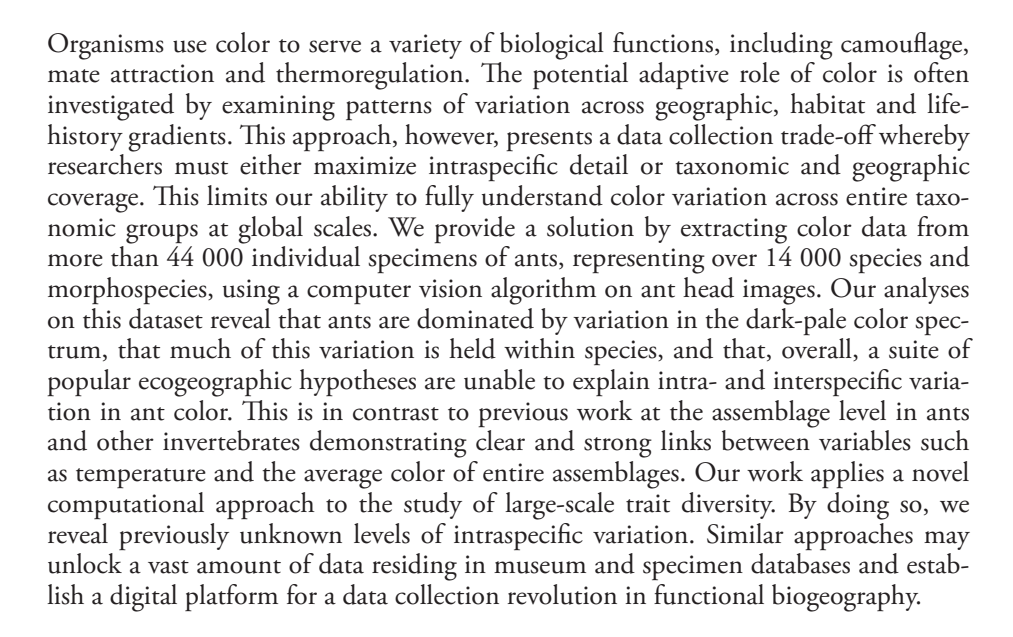
Correspondence: Jacob H. Idec (jacob.idec@ufl.edu); Tom R. Bishop (BishopTR@cardiff.ac.uk)

Ecography **2023:** e06279

doi: 10.1111/ecog.06279

Subject Editor: Sarah Diamond Editor-in-Chief: Miguel Araújo Accepted 28 November 2022





Keywords: ants, biogeography, color, computer vision, macroecology, traits

Introduction

From feathers to frogs to fungi, the color of organisms varies. This variation can depend on the interactions that organisms have with each other or with their environments. Birds of paradise use plumage color to attract a mate, an example of sexual selection, while poison arrow frogs advertise their toxicity with bright skin colors (Cuthill et al.



www.ecography.org

© 2023 The Authors. Ecography published by John Wiley & Sons Ltd on behalf of Nordic Society Oikos

This is an open access article under the terms of the Creative Commons Attribution License, which permits use, distribution and reproduction in any medium, provided the original work is properly cited.

wiley.com/doi/10.1111/ecog.06279 by EBMG ACCESS - MADAGASCAR, Wiley Online Library on [24/01/2023]. See the Terms and Conditions (https://onlinelibrary.wiley.com/terms-and-conditions) on Wiley Online Library for rules of use; OA articles are governed by the applicable Creative Commons License

¹Florida Museum of Natural History, Univ. of Florida, Gainesville, FL, USA

²School of Biosciences, Cardiff Univ., Cardiff, UK

³Dept of Zoology and Entomology, Univ. of Pretoria, Pretoria, South Africa

⁴Dept of Entomology, California Academy of Sciences, San Francisco, CA, USA

2017). A range of different taxa use color to camouflage themselves both actively (Hanlon 2007) and passively (Marshall et al. 2015) within their environment. Color also allows organisms to better exploit the abiotic conditions in which they find themselves. For example, dark colors enable fungi (Cordero et al. 2018), ants (Bishop et al. 2016), bird eggs (Wisocki et al. 2020) and lizards (Clusella-Trullas et al. 2007) to increase their heating rates in cool environments. These taxonomically and geographically widespread reports suggest that color may influence the ecology and evolution of a large fraction of biodiversity. Consequently, understanding color variation, and its evolutionary and ecological causes, will generate powerful insights into the past (Cuthill et al. 2017) and future of biodiversity (Bishop et al. 2019).

An emerging body of research recognizing the importance of color describes geographic patterns in color variation. Gloger's rule (Delhey 2017a) states that more heavily pigmented (darker) organisms are more likely to occur in warmer and more humid environments. This rule is focused on endotherms and finds support among various species and populations of mammals (Kamilar and Bradley 2011, Cerezer et al. 2020), birds (Burtt Jr and Ichida 2004, Roulin and Randin 2015) and even plants (Koski and Ashman 2015). While the mechanisms underlying Gloger's rule vary, in insects, a version of the rule called the photoprotection hypothesis (PPH) has been used to explain the presence of darker ants in high UV-B environments. In this case, the increased melanization of the ant cuticles is hypothesized to act as a sunscreen against tissue-damaging UV-B radiation (Bishop et al. 2016, Law et al. 2020). On the other hand, the thermal melanism hypothesis (TMH), sometimes referred to as Bogert's rule (Bogert 1949), is usually applied to ectotherms. The TMH states that organisms should be darker in colder environments because dark colors absorb more incoming solar radiation than pale colors, allowing animals to heat up and achieve operative temperatures more quickly (Clusella-Trullas et al. 2007). Evidence for the TMH has been found in ants (Bishop et al. 2016), dragonflies (Zeuss et al. 2014), butterflies (Heidrich et al. 2018), fungi (Cordero et al. 2018), birds eggs (Wisocki et al. 2020) and a range of reptiles (Clusella-Trullas et al. 2007). Together, these studies highlight how geographic variation can reveal important ecological principles.

Despite this progress, however, there is a major data collection trade-off that limits the generality of our understanding of the numerous roles that color plays in ecology and evolution. Researchers can opt to collect either high-resolution intraspecific information, or data across a broad taxonomic and geographic scope. For example, datasets capturing intraspecific variation are often focused on single species (Romano et al. 2019) or small geographic regions (Marshall et al. 2015). By contrast, datasets that explore variation across many species within a given evolutionary radiation (Delhey et al. 2019, Cerezer et al. 2020), or which cover large parts of the globe (Zeuss et al. 2014, Bishop et al. 2016), usually fail to capture intraspecific variability. This trade-off in data collection strategy has long been necessary because researchers have limited resources. Regardless, the trade-off means that we are largely

blind to the intraspecific variability that lies beneath broad geographic gradients of organismal color, and to the wider biogeographic context that surrounds in-depth studies of single species. In practice, it remains unclear whether patterns in color variation at the assemblage-level (Zeuss et al. 2014, Bishop et al. 2016) are matched by patterns in inter- and intraspecific variation. If patterns in color variation are similar across these different ecological levels, it would suggest that common mechanisms control both the survival of individuals and the structuring of entire assemblages (Gaston et al. 2008, Delhey 2017b). If not, then our understanding of trait-based ecology becomes more complicated.

Digitized specimen-level databases have the potential to break the data collection trade-off described above by offering specimen-level, intraspecific data at both taxonomically and geographically broad scales. The database AntWeb.org, which contains ~750 000 specimens, ~47 000 of which are represented by high-quality images that have been geolocated and taxonomically identified, provides an unparalleled and untapped opportunity to assess the global scale color variation of a particularly diverse family of insects. Ants (Order Hymenoptera, Family Formicidae) are a species-rich and eusocial group of insects found on all continents except Antarctica and in a variety of environmental conditions. As previously mentioned, emerging data suggest that the TMH (darker where cold) and the PPH (darker with high UV-B) operate in this group at the assemblage level (Bishop et al. 2016, Law et al. 2020). By using the data in AntWeb, we will be able to test these hypotheses even further. For example, ants living in different habitat strata (i.e. subterranean versus canopy) are exposed to vastly different environmental conditions which will presumably influence the selective forces operating on their color. For instance, we would expect the strength of the TMH and PPH to be greatly reduced in subterranean ants not directly exposed to sunlight. AntWeb provides a unique opportunity to collect paired data on ant specimen color and habitat strata preference, and to link these data to existing ecogeographic hypotheses.

Here, we develop a set of automated methods to use computer vision to extract color, caste and habitat strata information from ~47 000 individual ant workers belonging to ~8000 species across the globe (Fig. 1). We combine these data with a genus-level ant phylogeny and open-access climatic datasets to ask two key questions relating to variation in ant color. First, how does ant color vary? Popular ecogeographic rules typically assume that the most important axes of color variation are the dark-pale gradients produced by melanin, but this has not been explicitly tested. Second, does intra- and interspecific variation in ant color conform to the predictions of various ecogeographic rules? Specifically, we test whether the TMH and the PPH operate across the globe within the ants. In addition, we test the melanismdesiccation hypothesis (MDH), which posits that increased melanization decreases the permeability of the insect cuticle, preventing individuals from drying out in arid environments (Kalmus 1941). We also test whether the length of time that the specimens in AntWeb have been in storage drives their

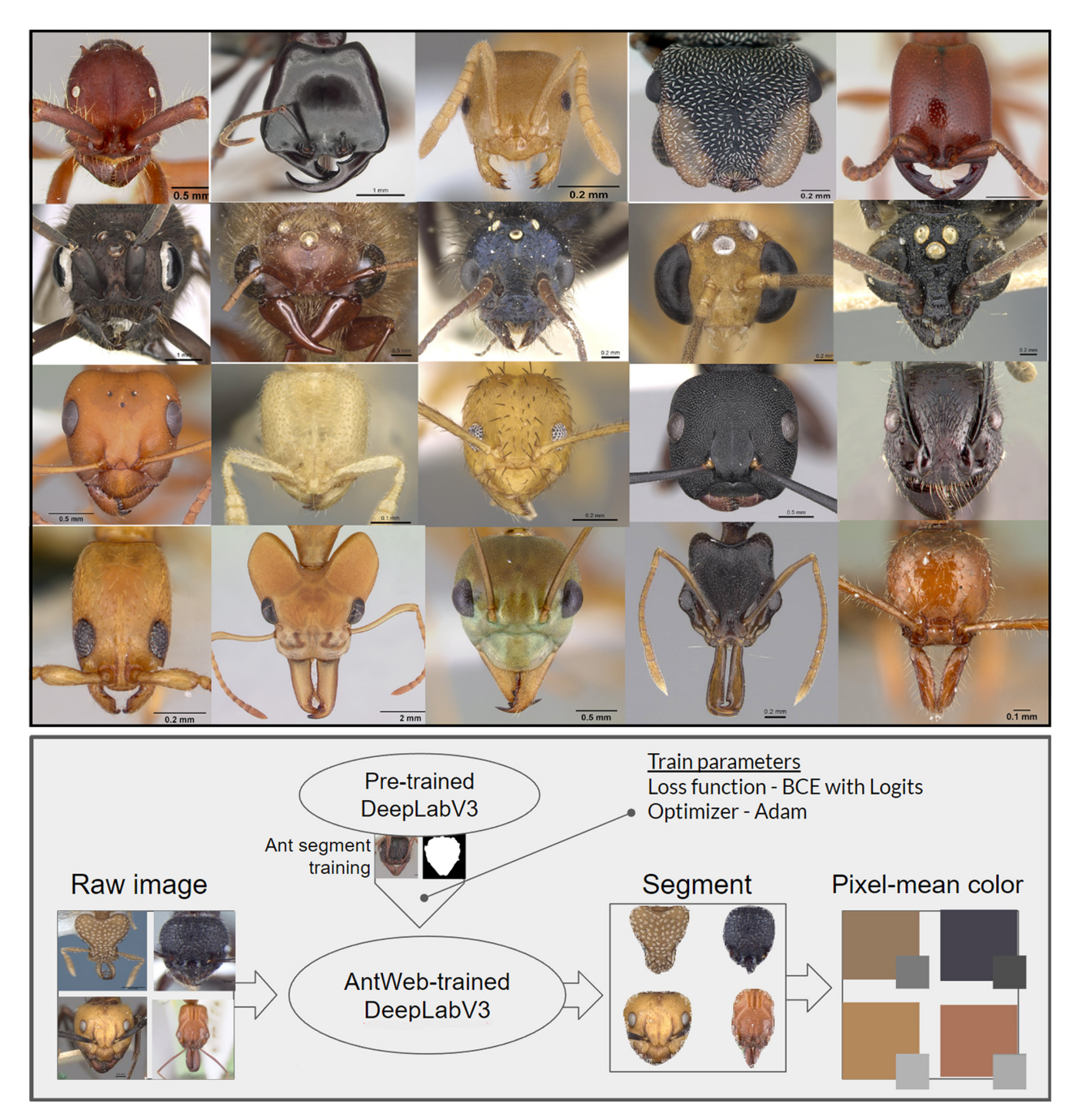


Figure 1. Above: Example images from AntWeb.org showing taxonomic, color, morphology and caste variation of the database. Below: Schematic diagram of the automated image segmentation procedure including training. Segments and colors shown were automatically extracted using the pipeline. Large squares show the mean RGB color of the segment pixels while grey squares show the mean HSV value component.

color patterns: we hypothesize that older specimens will fade and discolor over time, which may explain color gradients within the database.

Material and methods

AntWeb.org

The database AntWeb.org was developed by Brian L. Fisher in 2002 and includes over 780 000 specimens, 47 000 of which have associated images (Fig. 1). Specimens are contributed by 24 data providers based at museums and universities across the globe. The University of Utah (234 121 specimen records) and the California Academy of Sciences (231 106 specimen records) have contributed the greatest number of specimen records. All ant genera and 83% of valid ant species and subspecies are represented, although differences exist in the number of specimens and images per taxon. On average, 69% of the species found in each biogeographic region are imaged (Supporting information). Specimen records include a variety of fields including identification, caste assignment, collection date, imaging date (where applicable), collection event coordinates and notes taken at the time of collection.

Images were taken using a Leica DF425 camera using the same image format settings under a Leica LED5000 HDI Dome Illuminator at the California Academy of Sciences. Images taken at other institutions used identical or similar equipment and all followed a standard protocol for AntWeb. (www.antweb.org/web/homepage/Imaging_Manual_ LAS38 v03.pdf). White balance was standardized using a sheet of white paper before imaging. Gain, saturation and gamma were adjusted from an standard set of values to best match the image color to the visible color of each specimen as assessed by eye. This should make imaged specimen colors more in line with human perceived colors, but variation in how different imaging personnel make these adjustments could add noise at the individual level that contributes to observed intraspecific variation (Fig. 3). Exposure, the amount of light allowed to hit the specimen, is manually adjusted to minimize the number of overexposed and underexposed pixels. This leads to more visible detail but prioritizes body details over more accurate color by adjusting all the pixels in an image to be slightly darker or lighter. Ants with sections much lighter or darker than their surroundings might have their overall color lightness slightly reduced or increased, respectively, by this exposure adjustment. We do not expect this effect to occur in a systematic or biased

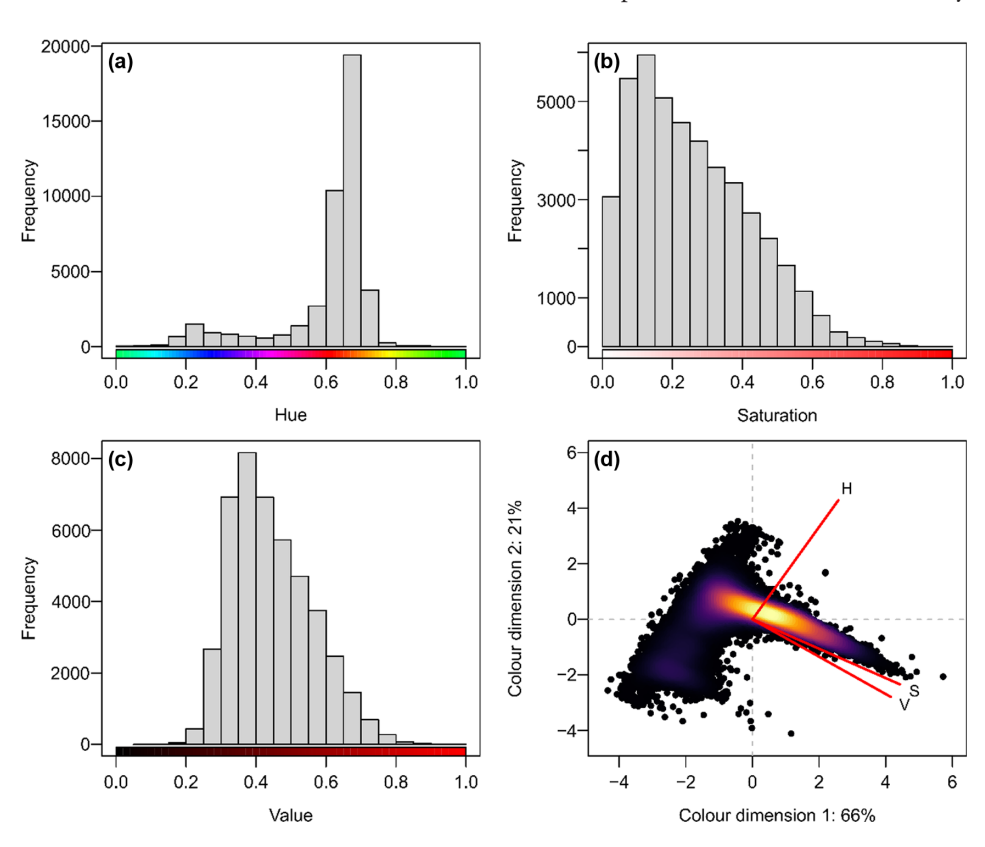


Figure 2. Distribution of hue (a), saturation (b) and value (c). Color bars under each histogram represent variation in each separate color component while keeping the other two components constant at either a hue of 0.6 (red), maximum saturation or maximum value. Panel (d) is a biplot of the PCA results summarizing global variation in ant specimen HSV. Points indicate individual specimens and are colored from black to white to emphasize point density. Red lines illustrate the loadings of the original HSV variables on the principal component dimensions. Dimension 1 is primarily associated with saturation (S) and value (V) variation, dimension 2 primarily with hue (H) variation. Percentage values refer to the total HSV variation that is captured by each dimension. Only the first two dimensions are shown here.

Species with high color variation Species with low color variation Lighter color Darker with low color variation Species with low color variation Pheidole crassinoda Labidus coecus

Figure 3. AntWeb.org images from four well-sampled species showcasing intraspecific variation as a combination of real color difference and random variation in imaging setup. Of the ~500 species containing ten or more specimens imaged, two species (left) were randomly selected from the 80th percentile of color variation (showing high intraspecific variation) and two species (right) were randomly selected from the 20th percentile (showing low intraspecific variation). For each species, ten random worker images are shown in order of descending lightness from the top. Colored squares next to each image show the color that was automatically extracted and used in analysis.

way across the imaged species, but it would make darker ants slightly lighter and lighter ants slightly darker, adding noise contrary to dark-to-light axis signal and increasing the risk of type-II error. However, our analyses still detected a strong dark-to-light axis, suggesting that the signal is visible through this exposure-adjustment noise.

Habitat strata assignment

We analyzed the text strings of the specimen 'collection-Notes' field to assign specimens to one of three habitat strata: hypogaeic (subterranean), epigaeic (ground-living) or arboreal (above ground-living). Approximately half of AntWeb specimens include 'collectionNotes,' which were taken by collectors at the time of collection, but none contain strict information on the habitat strata where they were collected. We searched the collection notes text strings for the presence of words and phrases indicative of habitat strata. For example, we interpreted 'soil core' as indicative of hypogaeic, 'ground forager' for epigaeic and 'above ground' for arboreal habitats. We also searched for the presence of words or phrases that exclude other words: for example, we interpreted the presence of 'tree' in the absence of 'fallen,' 'dead' or 'rotten' to indicate arboreal habitat. We assigned a habitat stratum to 254 492 out of the 400 000 specimens containing the 'collectionNotes' field (not all necessarily had images) using 32 different string conditions (Supporting information).

Color extraction

We developed a pipeline in Python and R to extract color information from AntWeb specimen imagery. The pipeline separates ants from their background, a process called segmentation, then quantifies the color of the ant by averaging its pixel RGB values (Fig. 1).

We first downloaded all 'medium' resolution specimen images from AntWeb, which allowed for faster analysis than the 'high' quality images while still maintaining color and visible detail. Each specimen in AntWeb has anterior, ventral side and dorsal side images. We quantified head color using the anterior images, which provide a frontal view of the head (Fig. 1 and 2). Only non-greyscale images were included, excluding color-invalid images such as SEM micrographs. For specimens with multiple anterior images we used the first image taken.

For our segmentation component, which extracts ant heads from the surrounding image (Fig. 1), we took an existing version of a DeepLabV3 ResNet101 pre-trained on a subset of the COCO Train2017 dataset and continued training it on our ant images in a process commonly known as transfer learning (Chen et al. 2017). Deep neural networks, most commonly with the segmentation architectures U-Net or DeepLab, have found increasing success for application on plant and insect specimens (Minakshi et al. 2020, Toulkeridou et al. 2020, Weaver et al. 2020). We trained the ant head segmenter using

50 randomly selected human-created ant masks each. Ten additional images were used in each test set, with half of these random and half chosen specifically to span ant head morphological diversity. Training used the ADAM optimizer and a binary-cross entropy with logits loss function. The images were resized to 344×344 pixels for segment training and mask inference, then the resulting mask was upscaled back to the initial image size. All model training and inference steps were performed using the Python library PyTorch.

We averaged all pixels of each segment by their RGB (red, green, blue) values and assigned this RGB value as the specimen head color. Finally, we used the rgb2hsv function in the R statistical programming environment to transform the RGB values of each specimen (described above) into HSV (hue, saturation and value) format, so that we could use the 'value' channel in our analysis (below). Our training data and all code for deep-learning segmentation and segment pixel averaging are freely available though a GitHub link within our Dryad repository.

We assessed the quality of our segmentation by randomly selecting 1000 segments and having an observer tag them as 'good,' 'include background,' 'head incomplete 75' or 'head incomplete 50.' Segments where greater than 10% of the area constituted background, antennae or thorax were tagged as 'include background,' a case where the mean color would be lighter than it should be because light background is captured. Images where this was not the case but the segment captured less than 75% or 50% of the ant's total head area were tagged as 'head incomplete 75' and 'head incomplete 50,' respectively. In these cases, mean color would not be derived from a full portion of the ant head, making it imperfect. All other segments were tagged as 'good.' Of the 1000 segments examined in this way, only ~1.5% of them were tagged as 'bad background' and ~0.5% of them were tagged as 'bad head incomplete 50,' representing a 2% rate of moderate error. An additional 1.5% were tagged as 'head incomplete 75,' which was considered a minor error.

We validated our pixel-averaged color estimates against those from a previously published method. Multiple studies on ants have quantified color via the human eye by scoring specimen color manually against a set of color references (Bishop et al. 2016, Law et al. 2020). We used the same set of reference colors as in those studies. Eight observers (the three authors plus five others) scored only the head images of between 30 and 139 randomly chosen ant specimens. We converted the manually scored colors into HSV color space. This left us with a dataset of color estimates on the same scale that had been captured by either our computer vision technique or by one of the eight human recorders. We used major axis linear regression on the raw and ranked lightness (V in HSV) data to understand how well the computer vision color estimates matched the manual method results.

Environmental and specimen data

We sourced data on mean annual temperature, mean annual precipitation, mean annual UV-B irradiance and specimen

storage duration for each specimen in our database. Mean annual temperature and mean annual precipitation were extracted for each specimen using latitude and longitude information from the WorldClim2 climatic layer (Fick and Hijmans 2017). We extracted UV-B radiation from the glUV climatic layer (Beckmann et al. 2014). UV-B also correlates strongly with temperature (Pearson's r = 0.64). This enabled us to take the residuals of the regression between UV-B and temperature as a measure of temperature-corrected ultraviolet radiation - high values indicate greater than expected UV for a given temperature, low values indicate lower than expected UV (Bishop et al. 2016). We calculated specimen storage duration as the difference in days between collection date and image upload date. In 1.4% of specimens the image upload date was prior to the specimen collection date - a typographical error. We assigned these specimens a storage duration of 0.

Statistical analysis

Ant color variation

We used a principal component analysis (PCA) to understand how the individual components (i.e. hue, saturation and value) of ant color covaried across the dataset. We scaled and centered the HSV data derived from our computer vision pipeline ('Color extraction,' above) before applying a PCA to them using the *princomp* function in R. Hereafter, our analyses focus on V (value) given its importance in ecogeographical hypotheses and refer to it as lightness.

We further analyzed the taxonomic and phylogenetic structure of ant color variation in two ways. First, we used a variance partitioning analysis to quantify the variation in ant color with respect to taxonomic rank. To do this, we constructed a linear mixed effects model using the *lme* function in the nlme package in R (Pinheiro et al. 2017, www.r-project.org). Lightness (i.e. V in HSV) was used as a response variable, and no fixed effects were used. The random effects were a nested hierarchy of subfamily, genus, species and caste (male, queen or worker). We applied the *varcomp* function from the package ape (Paradis and Schliep 2019) to this model to extract the variance components associated with each taxonomic rank. This approach follows that of Messier et al. (2010).

Second, we used a genus-phylogeny (Nelsen et al. 2018) to estimate the phylogenetic signal in lightness. We calculated the phylogenetic signal metrics Pagel's λ (Pagel 1999) and Blomberg's K (Blomberg et al. 2003) in two ways. First, we calculated phylogenetic signal with genus-level averages of value using the *phylosig* function of the phytools package (Revell 2012). Second, we incorporated species and specimen color variation by using the *intra_physig* function of the sensiPhy package (Paterno et al. 2018). This method incorporates variation within clades of a phylogeny (in our case, specimen-level variation within genera) by recalculating the phylogenetic signal metrics after drawing random values 1000 times from the distributions of the genus-level standard deviations.

We also used ancestral character state reconstruction (Revell 2013) to visualize how lightness varied across the ant phylogeny. We first split lightness into quartiles to aid the interpretation of this visualization, and then used the 'contMap' function of the phytools package in R (Revell 2012) with the default parameters to estimate the reconstruction.

Interspecific patterns

We used a multi-model inference framework to assess the evidence for or against three major ecogeographic rules relating to ectotherm color. These were the thermal melanism hypothesis (TMH, lighter colors where warm), the photoprotection hypothesis (PPH, lighter colors where relatively low UV-B) and the melanism-desiccation hypothesis (MDH, lighter colors where wet). We constructed three linear mixed models using the *nlme* package in R (Pinheiro et al. 2017). Each model represented one of the hypotheses. While these hypotheses are not strictly mutually exclusive (Wisocki et al. 2020), we opt to test them separately here for clarity. The fixed effects structure of the models was of the form:

Lightness $X \times \text{caste} \times \text{strata} + \text{storageduration} \times \text{caste} \times \text{strata}$

where X was either mean annual temperature (TMH), the residual UV-B irradiation (PPH) or mean annual precipitation (MDH). We included specimen storage duration and its interactions with caste and strata assignment in each model as a moderating variable - we expected that storage duration might influence specimen lightness, but were primarily interested in evaluating the relative effects of temperature, UV-B and rainfall. We included an exponential correlation structure into the models to account for potential spatial autocorrelation between specimens. We chose an exponential correlation structure because it had the lowest AIC compared to other structures. We controlled for the effect of ant phylogeny by including a nested random effect of species nested within genus within subfamily. We chose this approach because our phylogenetic data is only available at the genuslevel, meaning that to model specimen-level data we would need to assign specimens as polytomies within species polytomies. We consider the taxonomic rank approach used here a pragmatic solution given the resolution of the available phylogenetic data. In the analysis, each datapoint was an ant specimen (of any caste) that had associated geographic and environmental data (n = 15 207). We scaled and centered all explanatory variables prior to analysis to make the final models easier to interpret (Schielzeth 2010). To evaluate the relative support and explanatory power for each hypothesis we ranked the models according to AIC, calculated their R²_m and R² values (Nakagawa and Schielzeth 2013) and interpreted their estimated effect sizes. We did not perform any further model selection.

Intraspecific patterns

To investigate whether any of the three hypotheses explained color variation for individual species, we chose widespread species from the full dataset and applied models similar to them as above. First, we used three criteria to select species from the wider dataset. These species needed to 1) be represented by at least 10 worker individuals, 2) have specimens that were separated from each other by a median distance of at least 100 km and 3) have at least 30% of their environmental data values be unique. These criteria ensured that we tested widespread species that were not all sourced from a limited number of WorldClim pixels. Our chosen thresholds for these criteria are arbitrary, but they appear to avoid selecting species which were only sampled from a limited number of sites but with high worker numbers in our preliminary testing. We used only worker specimens in this analysis.

The selection criteria left us with 173 widespread species (average number of specimens per species = 14.39, minimum = 10, maximum = 60). For each of these species we used generalized least squares models from the nlme package in R (Pinheiro et al. 2017) to estimate how color lightness varied with respect to temperature (TMH), residual UV-B (PPH) and precipitation (MDH). For each species, we constructed a model with one of these environmental variables and specimen storage duration as the explanatory variable. Specimen lightness was used as the response variable. Each datapoint was a single worker ant specimen. As in the interspecific analysis, we included an exponential correlation structure in the models to account for potential spatial autocorrelation between specimens. For each modelled species, we extracted the estimated effect (± 95% CIs) of each explanatory variable and visualized these in a forest plot. We scaled and centered all explanatory variables prior to analysis (Schielzeth 2010).

Results

We extracted color data for 44 340 ant specimens. Of these, 21 001 had associated geographic coordinates and 9151 had collection information from which we could extract habitat strata information. When comparing the computer vision color estimation to the manual color estimation method (Bishop et al. 2016, Law et al. 2020), the manual method tended to overestimate extreme lightness values relative to the computer vision method (Supporting information). When comparing the lightness ranking of specimens between the two methods, however, we uncovered a 1:1 relationship for all observers (intercepts of 0 and slopes of 1, R2 values of 0.57-0.76, Supporting information). In other words, the computer vision method produces rankings of lightness similar to the manual method. Consequently, we expect that this method is not systematically biased compared to previously published methods.

Ant color variation

Across all ant specimens, the average hue was $0.60~(\pm~0.14~\rm SD)$, red on our rescaled hue variable), the average saturation was $0.25~(\pm~0.16~\rm SD)$ and the average value was $0.44~(\pm~0.12~\rm SD)$ (Fig. 2a–c).

The PCA on the HSV data produced three orthogonal dimensions of color variation. They captured 66, 21 and 12% of the total ant color variation, respectively. The first dimension (Fig. 2d) has high positive loadings for saturation (0.61) and value (0.60), and a slightly weaker positive loading for hue (0.52). Consequently, this first dimension largely describes variation from dark, weakly saturated ants to light, highly saturated ants. The second dimension almost exclusively captures variation in hue, from green-blue to orangeyellow. It has a high positive loading for hue (0.85) and weak negative loadings for saturation (-0.32) and value (-0.40). The third dimension describes the covariation of saturation and value. Saturation is strongly negatively loaded on this dimension (-0.72) while value is strongly positively loaded (0.69). This pattern is opposite to that captured by the first dimension, and describes variation from highly saturated but dark ants, to weakly saturated pale ants. Hue has a loading of 0 on this dimension.

The variance partitioning analysis revealed that 55% of the variation in specimen lightness (value) was held at intraspecific levels. 3.9% of the total variation was held between subfamilies, 22.06% was held between different genera within the same subfamily, 18.79% was held between different species within the same genus, 16% was held between different castes of the same species and 39% was held within the same caste of the same species. The variability of lightness within workers of the same species itself, however, varied across species (Fig. 3). The coefficient of variation for species with 10 or more specimens ranged from > 1% (little intraspecific variation) to greater than 140% (high intraspecific variation). Most species (75%) had a coefficient of variation in lightness > 30%. We found similar results, with high levels of intraspecific variation, in hue and saturation (Supporting information).

The phylogenetic signal analyses matched the variance partitioning results. Using only genus-level averages, and without including variation below the genus level, we detected a strong phylogenetic signal ($\lambda = 0.56$, p < 0.01; K=0.74, p < 0.01). When we included within-genus variation, however, the estimate of Pagel's λ was smaller but no longer significant ($\lambda = 0.15$, p=0.2), while the estimate of Blomberg's K was similar and still statistically significant (K = 0.62, p = 0.02). This analysis reflects the ~74% of lightness variation held below the genus level. Consequently, these results highlight that at the subfamily and genus level there is a strong phylogenetic signal in lightness in ants - closely related clades tend to be similar in terms of lightness (Fig. 4). This signal is eroded, however, when the large amount of species- and specimen-level variability is included.

Clear differences in lightness can be seen across the ant phylogeny: subfamily Ponerinae is largely dark, Myrmicinae is variable but with many pale genera, and the early branching subfamilies Martialinae, Proceratiinae, Apomyrminae and Leptanillinae tend to be pale. Further, the three largest subfamilies (Myrmicinae, Formicinae and Dolichoderinae) have groups of genera with either dark or pale coloration (Fig. 4).

Interspecific patterns

The model representing the TMH had the strongest support (Table 1). This model had the lowest AIC value, the largest R 2 _m and the largest effect size for its main effect (in this case, mean annual temperature). Further, this model revealed that ant specimens were generally paler in warmer conditions, matching the predictions of the TMH. The relationship between temperature and lightness was stronger for male ants than for queens and workers (Fig. 5a–c, p < 0.01, full model outputs in appendix) but did not appear to differ with respect to habitat strata (p > 0.05). This model also predicted a negative relationship between lightness and specimen storage duration (p < 0.01) such that specimens that had been in storage longer tended to have darker cuticles. This relationship was weaker for workers however than for males and queens (p < 0.01).

The second-best supported model was the one representing the PPH (Table 1). The lightness of queens and males displayed no relationship with residual UV-B, but workers became darker with increased UV-B (Fig. 5d–f, p=0.047). Similar specimen age effects were recovered as in the TMH model.

The model representing the MDH was the least well supported. This model had the largest AIC, the smallest $R_{\rm m}^2$ and the smallest main effect size (Table 1). The model found no significant association between lightness and mean annual rainfall (p > 0.05). There were also no significant associations with the interacting effects of caste and strata (Fig. 5g–i). Consequently, the predicted effects of the MDH were not met. Again, the predictions for storage duration were similar to that for the TMH model.

Each model had an R_m^2 of 2–3% and an R_c^2 of 59% (Table 1). Consequently, only a tiny fraction of variation in specimen lightness is explained by each of the models. The majority of variation is explained by the random effects accounting for ant phylogeny.

Intraspecific patterns

Overall, intraspecific variation in ant color did not clearly support any of the four hypotheses represented by the statistical models (Fig. 6). This conclusion comes from two lines of evidence from within the analysis. First, for each of the hypotheses most of the 173 species tested displayed no significant relationship (TMH = 13.3% of species were significant, PPH=12.7%, MDH=12.1%). Second, even where there were significant associations between lightness and the explanatory variables, the likelihood of these matching the predicted direction of the three target hypotheses effects was equivocal. For instance, the TMH predicts a positive relationship between lightness and temperature but only 56% of the significant species matched this (i.e. black points above the dashed line in Fig. 6). Similarly, the PPH predicts a negative relationship (59% of species) and the MDH predicts a negative relationship (42% of species). Consequently, our data reveal highly idiosyncratic and

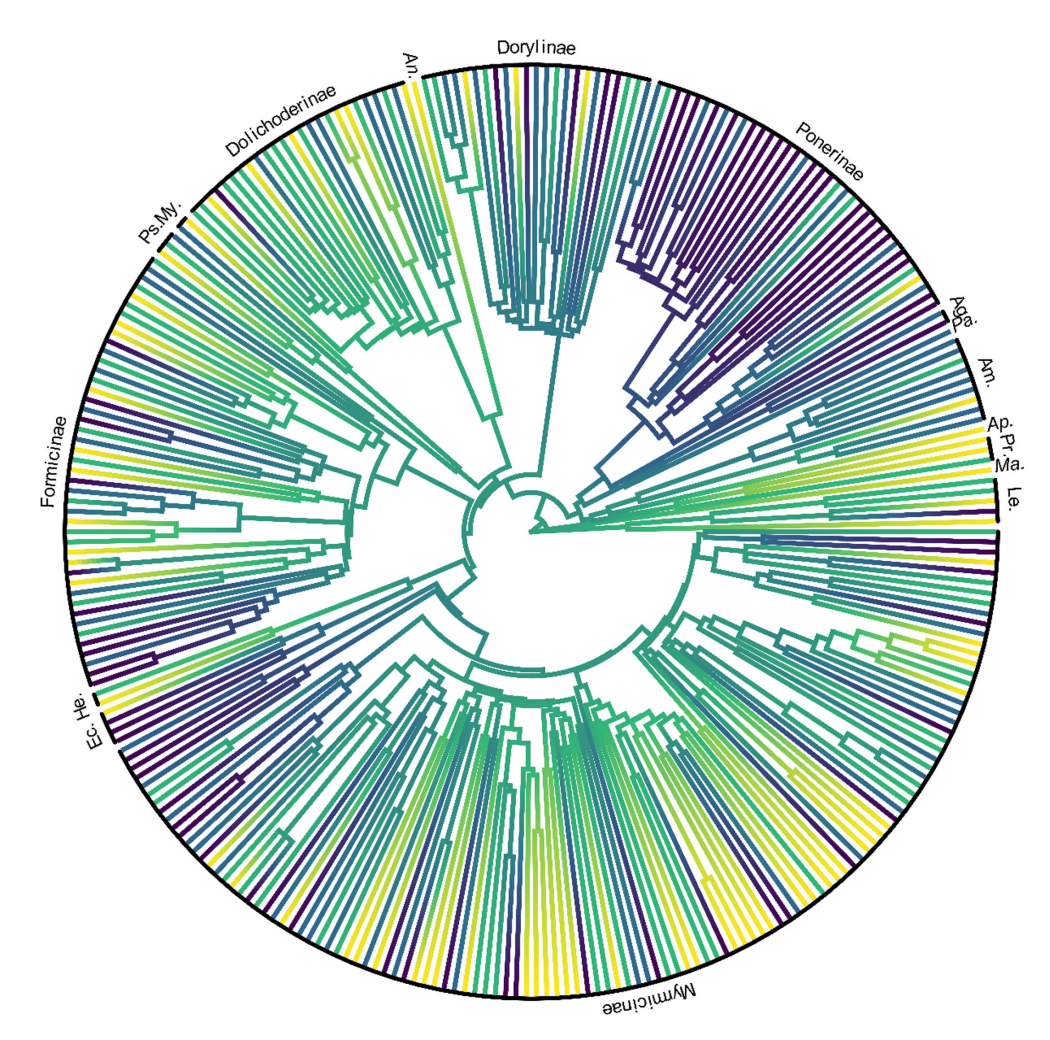


Figure 4. Genus-level phylogeny of the ants adapted from Nelsen et al. (2018). Dark colors (purple) represent clades which have dark coloration. Light colors (yellow) represent clades that have pale coloration. Subfamilies are labeled in full or abbreviated as follows: Ag. = Agroecomyrmecinae, Am. = Amblyoponinae, An. = Aneuretinae, Ap. = Apomyrminae, Ec. = Ectatomminae, He. = Heteroponerinae, Le. = Leptanillinae, Ma. = Martialinae, My. = Myrmecinae, Pa. = Paraponerinae, Pr. = Proceratiinae, Ps. = Pseudomyrmecinae.

species-specific associations between color lightness and the three candidate hypotheses. There is no general support at the intraspecific level for any of the hypotheses tested. Finally, these intraspecific effects did not appear to vary systematically with a suite of moderator variables including sample size, the variability of lightness or the geographic or environmental distance captured by each species within our dataset (Supporting information).

Discussion

Using a global dataset of specimen-level color, we show that ants mainly vary from dark to pale, that the majority of color variation is held at the intraspecific level and that three popular ecogeographic hypotheses cannot explain the majority of interspecific or intraspecific variation in ant color. This finding contrasts with existing analyses on ants at the

Table 1. Summary of linear mixed model outputs for the interspecific analysis. Models describe the relationship between color lightness and one of the focal explanatory variables while controlling for specimen storage duration. Models are ranked by AIC. TMH=thermal-melanism hypothesis, PPH=photoprotection hypothesis, MDH=melanism-desiccation hypothesis. LL=log likelihood. R_m^2 =marginal R^2 (variation explained by fixed+random effects), estimated effect=the estimated parameter of the main effect in the model (temperature, residual UV-B or rainfall) on the same standardized scale.

	· 1		-			
Hypothesis	AIC	ΔAIC	LL	R_{m}^{2}	R_{c}^{2}	Estimated effect
TMH	-28 889.8	0	14 467.96	0.03	0.59	0.02 ± 0.008
PPH	-28 854.5	35.3	14 450.31	0.03	0.59	0.0038 ± 0.0072
MDH	-28 842	47.85	14 444.03	0.02	0.59	0.00032 ± 0.0073

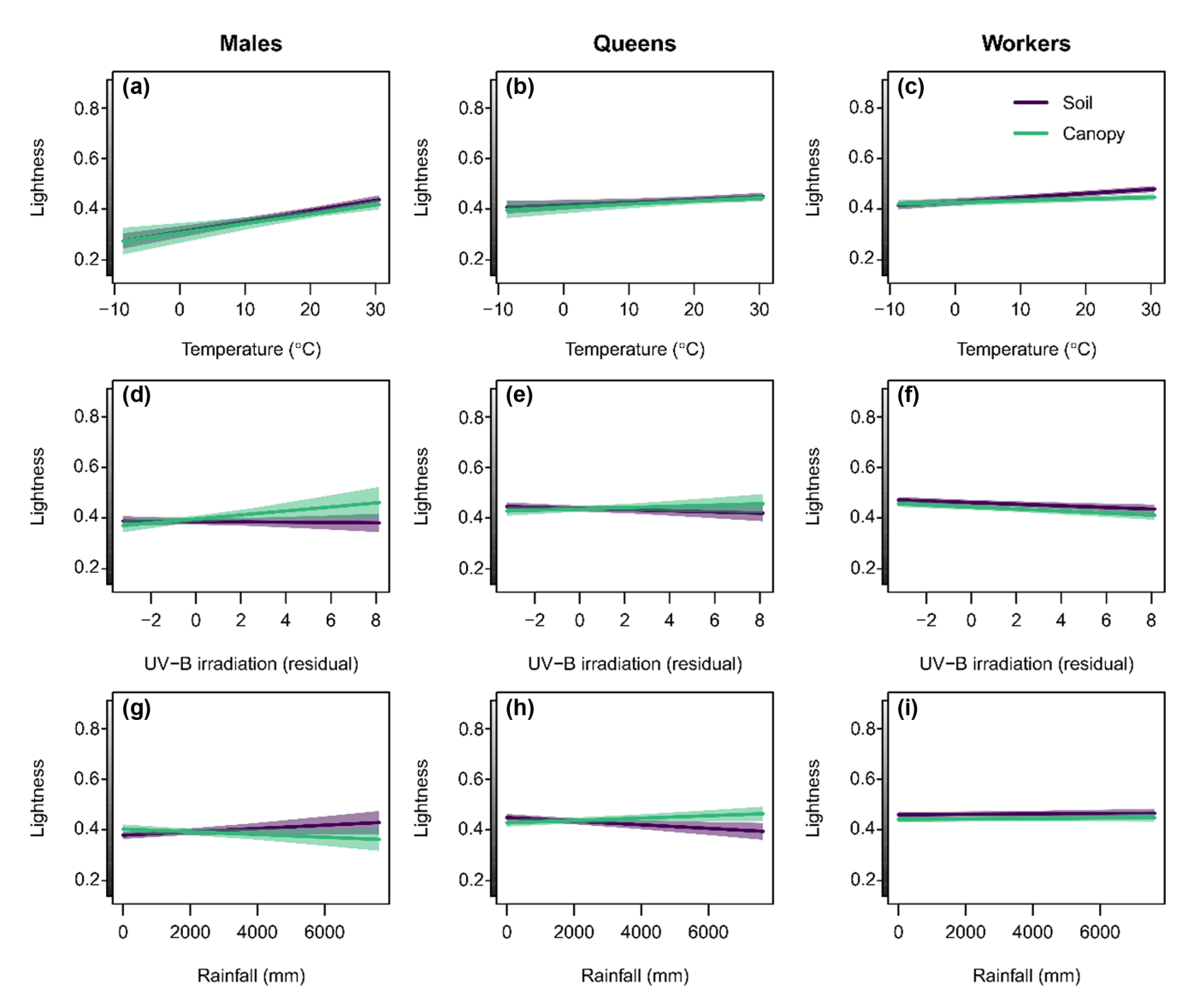


Figure 5. Interspecific analysis. Plots showing the predicted effects (lines) of temperature (top row, a–c), UV-B (middle row, d–f) and rainfall (bottom row, g–i) on specimen lightness. Green (paler) lines represent predictions for canopy specimens and purple (darker) lines represent predictions for soil specimens. Each panel shows predictions for either males (a, d, g), queens (b, e, h) or workers (c, f, i). Greyscale bar on y-axes represents actual changes in specimen lightness. Predictions related to specimen storage duration are presented in the appendix.

assemblage-level. We anticipate that our computer vision-based approach (Fig. 1) will have major consequences for the way in which functional biogeographers access and collate large-scale trait databases moving forward.

Our data provide the first quantitative evidence for the dominance of the dark-pale color spectrum among the ants. The major ecogeographic hypotheses relating to organismal color implicitly assume that variation between dark and pale colors is most important (Clusella-Trullas et al. 2007, Delhey 2017a). Our PCA analysis shows that this is indeed the case in the ants (Fig. 2): 66% of all HSV variation was associated with changes from dark (low S and V) to pale (high S and V). Changes in hue (i.e. blue, red, green, etc.) were largely associated with the second principal component axis, which accounted for only 21% of the total variation (Fig. 2).

Consequently, our data validate previous studies on ant color which have focused on color lightness at the expense of variation in hue (Bishop et al. 2016, Law et al. 2020). Given the large number of species we sampled, our results suggest that the dominance of the pale-dark spectrum may also exist in other holometabolous insect groups (Zeuss et al. 2014, Stelbrink et al. 2019). Given the available data, similar principal component analyses could be run in these groups to confirm this pattern. The real strength of our finding, however, is that it comes from the largest possible sample of ant color: our database contained color data from 44 340 individual specimens from across the globe, suggesting that the dominance of the dark-pale spectrum is a real biological pattern.

Further, variation in lightness (i.e. V in HSV) is taxonomically and phylogenetically structured in interesting ways.

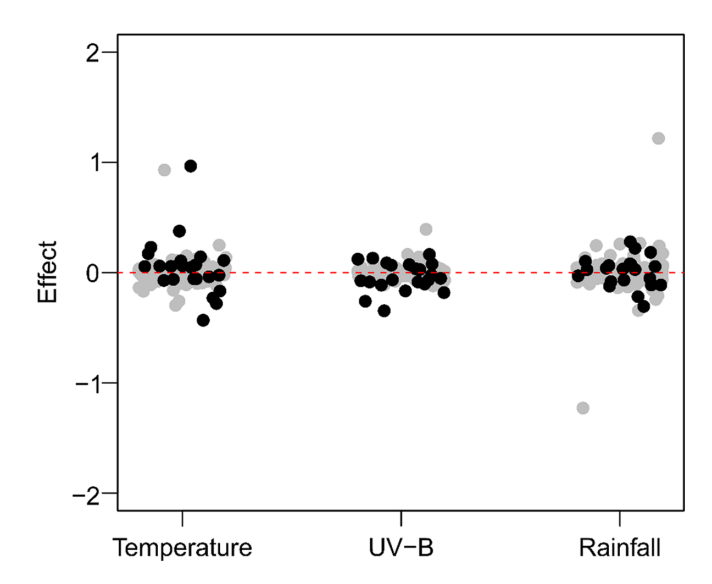


Figure 6. Plot showing the estimated effect (y-axis) of each of the candidate hypotheses (x-axis) on intraspecific color lightness. Each point represents the estimated effect for a single species and a given species (n=173) is represented by each of the three effects (total points = $172 \times 3 = 516$ datapoints in the plot). Grey points represent non-significant effects (where the 95% confidence intervals of the effect cross zero) and black points represent significant effects. Plots with CIs displayed are presented in the Supporting information. Significant effects are approximately evenly distributed between positive and negative effects. Theory predicts a positive effect for temperature, and a negative effect for UV-B and rainfall. Dashed red line indicates an effect of zero.

Our data show that lightness variation was split almost evenly between interspecific levels (between subfamilies, between genera and between species: 3.9+22+18.8=44.7%) and intraspecific levels (between castes and within castes of a species: 16+39.2=55.2%). This intraspecific fraction had a large influence on our phylogenetic signal analyses. When averaging away specimen-level variation and analyzing genuslevel variation, we found a significant phylogenetic signal. For example, the ponerine clade tends to be dark, while the myrmecines are primarily light but have repeatedly evolved darkly colored genera (Fig. 4). Once the between- and within-species variation has been accounted for, however, this phylogenetic signal becomes insignificant - emphasizing that the full spectrum of lightness variation can be found almost anywhere on the ant phylogeny when looking at individual species or specimens. Intraspecific variation in ant and insect color is understudied (but see Hegna et al. 2013), but previous work on ant morphological traits has found that intraspecific variability among workers of the same caste is typically low at around 1-4% depending on the trait (Gaudard et al. 2019). Consequently, the data we present here suggest that color lightness is more variable in ants (i.e. 39% of total lightness variability is found within castes) than other aspects of their morphology. Therefore, researchers studying color across large taxonomic or geographic scales should attempt to account for intraspecific variation in their analyses.

The large intraspecific variation in ant color that we report also raises the question of its cause. Here, we tested three popular ecogeographic hypotheses at the intraspecific and interspecific level. None of them provided general explanations for intraspecific variation in ant color. In fact, the majority of the widespread ant species that we analyzed displayed no evidence of significant, systematic trends in their lightness variation (Fig. 6). While a minority of species displayed significant associations between lightness and at least one of the hypothesized drivers, the direction of these effects was equally likely to be positive or negative (Fig. 5). For example, our data show that species are equally likely to match to the thermal melanism hypothesis (lighter where warmer) as they are to display opposite patterns (lighter where colder). Consequently, our largescale, comparative data are unable to explain why ant workers of the same species vary in their color. We note that individual reports exist whereby intraspecific variation in ant color appears to match one or more of these major ecogeographical hypotheses (Branstetter 2013). We do not cast doubt on these examples. Instead, we highlight the bigger picture within which these cases fit: different species are likely responding to completely different selective pressures on their color lightness, and these pressures may or may not be linked to the dominant ecogeographical hypotheses outlined in the literature to date.

At the interspecific-level, the model representing the thermal-melanism hypothesis offered the best fit (Table 1, Fig. 5a-c). This is consistent with previous research on ant thermal ecology. Temperature has been shown to influence ant activity (Jayatilaka et al. 2011), the diversity and distribution of species (Sanders et al. 2007, Warren and Chick 2013) and color across thermal gradients at the assemblage level (Bishop et al. 2016). In our dataset, ants are paler at higher temperatures, as predicted by the thermal-melanism hypothesis. We anticipated finding a stronger thermal melanism effect for canopy ants compared to ground-living ants, but this was not the case. The thermal-melanism hypothesis is centered on the effect of incoming solar radiation landing on ectotherm bodies (Clusella-Trullas et al. 2007). As ants living within the soil column itself are largely shielded from solar radiation, we would not expect the thermal-melanism hypothesis to affect them. Ground- and canopy-living ants, however, are much more likely to be exposed to the sun's rays, and to conform to the thermal-melanism hypothesis. Yet our data do not match this expectation, echoing the results of Heidrich et al. (2018). Heidrich et al. (2018) found that both diurnal and nocturnal moths conformed to the expected geographic patterns of the thermal-melanism hypothesis. Heidrich et al. (2018) propose that this may be because melanization is correlated with several other morphological and developmental traits. In particular, increased melanization has been linked to increased development time (Talloen et al. 2004). In cold environments, ectotherms typically develop at a slower rate than in warm environments (Sibly and Atkinson 1994). Consequently, the darker colors of the subterranean ants we find in cool environments may be caused by the slower rate of development that occurs in these places, rather than a thermoregulatory mechanism per se.

Our analysis also suggests that temperature generally exhibits a stronger selective pressure on ant coloration than UV-B. While we found a significant negative relationship between worker lightness and UV-B (the photoprotection hypothesis or Gloger's rule), this model was clearly ranked second in comparison to the TMH and had much smaller effect sizes (Table 1). There are exceptions, however. Approximately half of the species tested at the intraspecific level had significant negative associations between lightness and UV-B - highlighting that species-specific ecology and life history has a major role in which ecogeographic rules may be 'obeyed'. Further, in local environments where temperature is relatively homogenous but where UV-B may vary strongly the PPH does seem to constrain color variation. Law et al (2020) found this effect across vertical gradients in tropical rainforest, albeit at the assemblage level.

A more important point to note when interpreting our models (Table 1), however, is that they explain only a small fraction of the total variability in our dataset. For example, in the best model, the TMH, the fixed effects explain only ~3% of the total variability in the dataset. The fixed effects and the random effects of taxonomic rank, however, explain 59% of the variability. Consequently, while we observed a clear signal of the TMH in our dataset (Table 1), the ability of this hypothesis to explain variation in ant color on its own is low. Much variation is locked up in the taxonomic effects of subfamily, genus and species. This contrasts with the relatively high R² values obtained by previous studies at the assemblagelevel. Bishop et al. (2016) found evidence for the TMH and the PPH, obtaining fixed effect R2s of ~50%. We hypothesize that this effect of different data scales may be general. The cuticle color of individual ant workers and species is likely subject to a range of different selection pressures and developmental and evolutionary constraints. Further, different species may well be thermoregulating, or responding to a variety of environmental pressures, without relying on cuticle color (Shi et al. 2015). This difference between species/individual and assemblage level analyses has also been found in birds, where the effect of various ecogeographic rules nearly always appears stronger when the data are aggregated at the assemblage level (Delhey 2017b). Birds also appear to display this pattern for body size, whereby entire bird assemblages appear to follow Bergmann's rule (larger where colder) (Olson et al. 2009) in contrast to individual species (Riemer et al. 2018).

Our findings demonstrate the value of a computer vision-aided approach to the study of trait biodiversity. However, there may be some limitations to our current implementation. For example, differently colored setae, cuticle reflectiveness, the quality of the image segmentation and oversaturated photographs may all contribute to noise within our dataset. We do not expect these factors to be differentially expressed between environments, castes or habitat strata to the point where they would affect our modelling results, however. Regardless, our approach using image analysis, online databases and text mining techniques could be applied to other taxonomic groups with large and well-curated databases. Image segmentation techniques are steadily improving and

adapting cutting edge algorithms will allow us to obtain increasingly accurate and high-resolution data from specimen images. This will include information not just about color, but a wide gamut of morphological data. This will broaden the possible set of biogeographical questions that we can answer (Violle et al. 2014). Image databases for a variety of taxa grow larger every day – LepNet already contains 255 000 imaged butterflies (Seltmann et al. 2017). Integrating intraspecific detail with biogeographical coverage will finally be attainable in any taxon with a large and well-curated image database, helping us to understand the evolution and ecology of traits across the globe.

Funding - TRB was supported by the Leverhulme Trust (ECF-2017-208).

Author contributions

Jacob H. Idec: Conceptualization (equal); Data curation (lead); Formal analysis (equal); Methodology (equal); Software (lead); Visualization (equal); Writing — original draft (equal); Writing — review and editing (equal). Tom R. Bishop: Conceptualization (equal); Formal analysis (lead); Methodology (equal); Visualization (equal); Writing — original draft (equal); Writing — review and editing (equal). Brian L. Fisher: Conceptualization (equal); Data curation (equal); Methodology (supporting); Resources (lead); Supervision (equal); Writing — review and editing (equal).

Transparent peer review

The peer review history for this article is available at https://publons.com/publon/10.1111/ecog.06279.

Data availability statement

Data are available from the Dryad Digital Repository: https://doi.org/10.5061/dryad.pvmcvdnqd (Idec et al. 2022).

Supporting information

The Supporting information associated with this article is available with the online version.

References

Beckmann, M., Václavík, T., Manceur, A. M., Šprtová, L., Wehrden, H., Welk, E. and Cord, A. F. 2014. glUV: a global UV-B radiation data set for macroecological studies. – Methods Ecol. Evol. 5: 372–383.

Bishop, T. R., Robertson, M. P., Gibb, H., van Rensburg, B. J.,
Braschler, B., Chown, S. L., Foord, S. H., Munyai, T. C., Okey,
I., Tshivhandekano, P. G., Werenkraut, V. and Parr, C. L. 2016.
Ant assemblages have darker and larger members in cold environments. – Global Ecol. Biogeogr. 25: 1489–1499.

Bishop, T. R., Parr, C. L., Gibb, H., van Rensburg, B. J., Braschler, B., Chown, S. L., Foord, S. H., Lamy, K., Munyai, T. C., Okey,

- I., Tshivhandekano, P. G., Werenkraut, V. and Robertson, M. P. 2019. Thermoregulatory traits combine with range shifts to alter the future of montane ant assemblages. Global Change Biol. 25: 2162–2173.
- Blomberg, S. P., Garland Jr, T., Ives, A. R. and Crespi, B. 2003. Testing for phylogenetic signal in comparative data: behavioral traits are more labile. Evolution 57: 717–745.
- Bogert, C. M. 1949. Thermoregulation in reptiles, a factor in evolution. Evolution 3: 195–211.
- Branstetter, M. G. 2013. Revision of the Middle American clade of the ant genus Stenamma Westwood (Hymenoptera, Formicidae, Myrmicinae). ZooKeys 295: 1–297.
- Burtt Jr, E. H. and Ichida, J. M. 2004. Gloger's rule, feather-degrading bacteria and color variation among song sparrows. Condor 106: 681–686.
- Cerezer, F. O., Ribeiro, J. R., Graipel, M. and Cáceres, N. C. 2020. The dark side of coloration: ecogeographical evidence supports Gloger's rule in American marsupials. – Evolution 74: 2046–2058.
- Chen, L.-C., Papandreou, G., Kokkinos, I., Murphy, K. and Yuille,
 A. L. 2017. Deeplab: semantic image segmentation with deep convolutional nets, atrous convolution and fully connected crfs.
 IEEE Trans. Pattern Anal. Mach. Intell. 40: 834–848.
- Clusella-Trullas, S., van Wyk, J. H. and Spotila, J. R. 2007. Thermal melanism in ectotherms. J. Therm. Biol. 32: 235–245.
- Cordero, R. J., Robert, V., Cardinali, G., Arinze, E. S., Thon, S. M. and Casadevall, A. 2018. Impact of yeast pigmentation on heat capture and latitudinal distribution. Curr. Biol. 28: 2657.e3–2664.e3.
- Cuthill, I. C., Allen, W. L., Arbuckle, K., Caspers, B., Chaplin, G., Hauber, M. E., Hill, G. E., Jablonski, N. G., Jiggins, C. D. and Kelber, A. 2017. The biology of color. – Science 357: eaan0221.
- Delhey, K. 2017a. Gloger's rule. Curr. Biol. 27: R689-R691.
- Delhey, K. 2017b. Darker where cold and wet: Australian birds follow their own version of Gloger's rule. Ecography 41: 673–683.
- Delhey, K., Dale, J., Valcu, M. and Kempenaers, B. 2019. Reconciling ecogeographical rules: rainfall and temperature predict global colour variation in the largest bird radiation. Ecol. Lett. 22: 726–736.
- Fick, S. E. and Hijmans, R. J. 2017. WorldClim 2: new 1-km spatial resolution climate surfaces for global land areas. Int. J. Climatol. 37: 4302–4315.
- Gaston, K. J., Chown, S. L. and Evans, K. L. 2008. Ecogeographical rules: elements of a synthesis. J. Biogeogr. 35: 483–500.
- Gaudard, C. A., Robertson, M. P. and Bishop, T. R. 2019. Low levels of intraspecific trait variation in a keystone invertebrate group. – Oecologia 4: 725–735.
- Hanlon, R. 2007. Cephalopod dynamic camouflage. Curr. Biol. 17: R400–R404.
- Hegna, R. H., Nokelainen, O., Hegna, J. R. and Mappes, J. 2013. To quiver or to shiver: increased melanization benefits thermoregulation, but reduces warning signal efficacy in the wood tiger moth. – Proc. R. Soc. B 280: 20122812.
- Heidrich, L., Friess, N., Fiedler, K., Brändle, M., Hausmann, A., Brandl, R. and Zeuss, D. 2018. The dark side of Lepidoptera: colour lightness of geometrid moths decreases with increasing latitude. – Global Ecol. Biogeogr. 27: 407–416.
- Idec, J. H., Bishop, T. R. and Fisher, B. L. 2022. Data from: Using computer vision to understand the global biogeography of ant color. – Dryad Digital Repository, https://doi.org/10.5061/ dryad.pvmcvdnqd.

- Jayatilaka, P., Narendra, A., Reid, S. F., Cooper, P. and Zeil, J. 2011. Different effects of temperature on foraging activity schedules in sympatric Myrmecia ants. – J. Exp. Biol. 214: 2730–2738.
- Kalmus, H. 1941. Physiology and ecology of cuticle colour in insects. Nature 148: 428–431.
- Kamilar, J. M. and Bradley, B. J. 2011. Interspecific variation in primate coat colour supports Gloger's rule. J. Biogeogr. 38: 2270–2277.
- Koski, M. H. and Ashman, T.-L. 2015. Floral pigmentation patterns provide an example of Gloger's rule in plants. Nat. Plants 1: 1–5.
- Law, S. J., Bishop, T. R., Eggleton, P., Griffiths, H., Ashton, L. and Parr, C. 2020. Darker ants dominate the canopy: testing macroecological hypotheses for patterns in colour along a microclimatic gradient. J. Anim. Ecol. 89: 347–359.
- Marshall, K. L., Philpot, K. E., Damas-Moreira, I. and Stevens, M. 2015. Intraspecific colour variation among lizards in distinct island environments enhances local camouflage. – PLoS One 10: e0135241.
- Messier, J., McGill, B. J. and Lechowicz, M. J. 2010. How do traits vary across ecological scales? A case for trait-based ecology. Ecol. Lett. 13: 838–848.
- Nakagawa, S. and Schielzeth, H. 2013. A general and simple method for obtaining R² from generalized linear mixed-effects models. Methods Ecol. Evol. 4: 133–142.
- Nelsen, M. P., Ree, R. H. and Moreau, C. S. 2018. Ant–plant interactions evolved through increasing interdependence. – Proc. Natl Acad. Sci. USA 115: 12253–12258.
- Olson, V. A., Davies, R. G., Orme, C. D. L., Thomas, G. H., Meiri,
 S., Blackburn, T. M., Gaston, K. J., Owens, I. P. and Bennett,
 P. M. 2009. Global biogeography and ecology of body size in birds. Ecol. Lett. 12: 249–259.
- Pagel, M. 1999. Inferring the historical patterns of biological evolution. Nature 401: 877–884.
- Paradis, E. and Schliep, K. 2019. ape 5.0: an environment for modern phylogenetics and evolutionary analyses in R. Bioinformatics 35: 526–528.
- Paterno, G. B., Penone, C. and Werner, G. D. 2018. sensiPhy: an r-package for sensitivity analysis in phylogenetic comparative methods. – Methods Ecol. Evol. 9: 1461–1467.
- Pinheiro, J., Bates, D., DebRoy, S., Sarkar, D. and R Core Team 2017. nlme: linear and nonlinear mixed effects models. R package ver. 3.1-159, https://CRAN.R-project.org/package=nlme.
- Revell, L. J. 2012. phytools: an R package for phylogenetic comparative biology (and other things). Methods Ecol. Evol. 3: 217–223.
- Revell, L. J. 2013. Two new graphical methods for mapping trait evolution on phylogenies. Methods Ecol. Evol. 4: 754–759.
- Riemer, K., Guralnick, R. P. and White, E. P. 2018. No general relationship between mass and temperature in endothermic species. eLife 7: e27166.
- Romano, A., Séchaud, R., Hirzel, A. H. and Roulin, A. 2019. Climate-driven convergent evolution of plumage colour in a cosmopolitan bird. Global Ecol. Biogeogr. 28: 496–507.
- Roulin, A. and Randin, C. 2015. Gloger's rule in North American barn owls. Auk Ornithol. Adv. 132: 321–332.
- Sanders, N. J., Lessard, J.-P., Fitzpatrick, M. C. and Dunn, R. R. 2007. Temperature, but not productivity or geometry, predicts elevational diversity gradients in ants across spatial grains. Global Ecol. Biogeogr. 16: 640–649.

- Schielzeth, H. 2010. Simple means to improve the interpretability of regression coefficients. Methods Ecol. Evol. 1: 103–113.
- Seltmann, K. C., Cobb, N. S., Gall, L. F., Bartlett, C. R., Basham, M. A., Betancourt, I., Bills, C., Brandt, B., Brown, R. L. and Bundy, C. 2017. LepNet: the Lepidoptera of North America network. – Zootaxa 4247: 73–77.
- Shi, N. N., Tsai, C.-C., Camino, F., Bernard, G. D., Yu, N. and Wehner, R. 2015. Keeping cool: enhanced optical reflection and heat dissipation in silver ants. Science 349: 298–301.
- Sibly, R. and Atkinson, D. 1994. How rearing temperature affects optimal adult size in ectotherms. Funct. Ecol. 486–493.
- Stelbrink, P., Pinkert, S., Brunzel, S., Kerr, J., Wheat, C. W., Brandl, R. and Zeuss, D. 2019. Colour lightness of butterfly assemblages across North America and Europe. – Sci. Rep. 9: 1–10.

- Talloen, W., Dyck, H. V. and Lens, L. 2004. The cost of melanization: butterfly wing coloration under environmental stress. Evolution 58: 360–366.
- Violle, C., Reich, P. B., Pacala, S. W., Enquist, B. J. and Kattge, J.
 2014. The emergence and promise of functional biogeography.
 Proc. Natl Acad. Sci. USA 111: 13690–13696.
- Warren, R. J. and Chick, L. 2013. Upward ant distribution shift corresponds with minimum, not maximum, temperature tolerance. – Global Change Biol. 19: 2082–2088.
- Wisocki, P. A., Kennelly, P., Rojas Rivera, I., Cassey, P., Burkey, M. L. and Hanley, D. 2020. The global distribution of avian eggshell colours suggest a thermoregulatory benefit of darker pigmentation. Nat. Ecol. Evol. 4: 148–155.
- Zeuss, D., Brandl, R., Brändle, M., Rahbek, C. and Brunzel, S. 2014. Global warming favours light-coloured insects in Europe. – Nat. Commun. 5: 3874.